COMPOSITE FILMS AS ALTERNATIVE PACKAGING FOR UV-LIGHT BARRIER INTENDED FOR FOOD PRESERVATION.

Authors: R.A. Batista, J.T. Faria, P.J.P. Espitia, N. Narain, N.F.F. Soares and E. Medeiros
Date: Dec. 2019
From: Italian Journal of Food Science(Vol. 31, Issue 6SI)
Publisher: Chiriotti Editori S.r.l.
Document Type: Article
Length: 3,934 words
Lexile Measure: 1480L

Abstract:

Food exposure to light result in oxidation. This study aimed to develop films as UV-light barrier using central composite design. Low density polyethylene films were incorporated with tinuvin and iron particles. Physical-mechanical properties (crystallinity, microstructure, mechanical resistance, color properties, thermal stability) and UV-light barrier were evaluated. Iron did no influence film's crystallinity; however, mechanical resistance was affected by iron. Microscopy analyses showed iron agglomeration on films surface. Films presented a maximum decomposition temperature (550.1 [+ or -] 8[degrees]C). Tinuvin and iron affected [L.sup.*], [a.sup.*], opacity and whiteness index. Only tinuvin had a significant effect on UV-light absorbed at 250, 3l0 and 360 nm wavelengths.

Keywords: food packaging, food preservation, UV light barrier

Full Text:

1. INTRODUCTION

Photo-induced oxidation is considered as one of the major causes of food degradation because it causes alterations in the intrinsic and extrinsic properties of food products in a short period of time, changing nutritional and organoleptic features of foods and reducing their shelf-life (GIBIS and RIEBLINGER, 2011). One of the prune causes of decreased food quality is food product exposition to light, which induces oxidation processes. Food products can be exposed to light on several phases of the food production-chain, such as processing, packaging, distribution retailing and storing, which eventually results in the photo-induced oxidation process (INTAWIWAT et al., 2012). Thus, in order to diminish photo-induced oxidation, opaque and nontransparent materials, such as aluminum foil, have been used as a method for reduction of light incidence in food products. Meanwhile the interest and demand for transparent packaging has increased recently in the food industry due to attempts to enhance and differentiate the food product image on the shelves. Moreover, awareness related to environmental contamination has resulted in a reduced use of aluminum and metallized foils (MORTENSEN et al., 2004).

On the other hand, food packaging has critical and essential functions required for ensuring food preservation, especially those related to food protection during transporting and storage (YILDIRIM et al., 2018). Therefore, innovations related to the development of active food packaging are in constant progress in order to control or minimize external factors that might affect food stability and accelerate food spoilage as a result of chemical reactions, physical changes, or microbial contamination (ESPITIA et al., 2012).

In this regard, active packaging with antioxidant properties has emerged to control photo-induced oxidation in food products (SAHRAEE et al., 2019). Active packaging can contain food with novel functions, which includes antimicrobial, antioxidant, antiwetting or flavoring properties (FARAONI et al., 2008). The

development of novel technology, and especially those related to the advancement of the food packaging field is a response to the emerging needs of the food industry and society, which take into consideration factors such as globalization of resources, which means increased distance among producers and consumers, current food regulations, and healthy life-style of consumers (YILDIRIM et al., 2018).

According to LEE et al. (2008), polyethylene (PE) has a vast market due to its versatility, transparency, high strength to chemical solvents, easy heat-sealing, barrier to moisture and low cost. According to Soares and Hotchkiss (1998), the combination of core technologies for food preservation and active packaging is essential to ensure food safety and increase the shelf-life of the packaged food product. Active packaging is a type of packaging that interacts intentionally with food in order to maintain the organoleptic and nutritional characteristics of the packaged product or even to improve them (RODRIGUEZ-ROJAS et al., 2019).

One of the active compounds that can be incorporated into PE matrix is tinuvin 326. Tinuvin is a benzotriazole used in the packaging industry as UV light absorber. It has low volatility at high temperatures, is resistant to thermal degradation and can be used without significant loss or decomposition during the extrusion of low-density polyethylene (LDPE) films (CIBA, 2002). Moreover, iron particles can be incorporated in food packaging in order to act synergistically with tinuvin and thus improve UV light barrier of films. This study was therefore aimed to develop LDPE films with UV light absorption properties. The LDPE films were incorporated with tinuvin and iron particles and the physical and mechanical properties of developed films were evaluated, including microscopic analysis, mechanical resistance, color properties, thermal stability and potential barrier to UV light. The films were developed using the central composite design (CCD) and data were analyzed with the statistical approaches of response surface methodology (RSM).

2. MATERIAL AND METHODS

The UV barrier films were prepared using low density polyethylene (LDPE, Braskem S.A., Triunfo, Rio Grande do Sul, Brazil) incorporated with Tinuvin 326 (chemical name: 2-(2'Hydroxy-3-tert-butyl-5-methylphenyl)-5-chlorobenzortriazole; CAS number 3896-11-5) supplied by Ciba-Brazil, and iron powder with particle size of 3 microns (99.67 % iron content) provided by Sigma-Aldrich, Sao Paulo, Brazil.

2.1. Film Elaboration

The UV barrier films were elaborated as follows: tinuvin 326 and iron powder (at different concentrations) were blended with the LDPE resin according to the CCD (Table 1).

Each mixture was processed in a twin-screw extruder (Thermo Electron Corporation, Model AX plastic) at 30 rpm of speed and provided with ten heating zones at 165, 170, 170, 175, 175, 175, 175, 180, 180 and 180[degrees]C, respectively. After this process, pellets of LDPE incorporated with Tinuvin and iron particles were obtained.

Following this, the UV barrier films were produced in a tubular shape by processing the obtained pellets in a single-screw extruder (Thermo Electron Corp., model HAAKE Polydrive R600/610, Karlsruhe, Germany) at 30 rpm speed and provided with five heating zones at temperatures of 130, 140, 150, 160 and 170[degrees]C.

2.2. Experimental Design and Statistical Analysis

The central composite design (CCD) was used to evaluate the combined effects of tinuvin and iron particles on the physical and mechanical properties of developed films. The experiment was planned according to the CCD, constituted by a factorial experiment ([2.sup.2]), with the concentration of tinuvin and iron particles being the independent variables. Moreover, the experiment was provided with four treatments in the axial points and three replicates in central point. The whole experiment resulted in 11 treatments (Table 1). The results were analyzed using the statistical approach of response surface methodology using the Statistical Analysis System version 9.1 (SAS Inc., Cary, N.C., U.S.A.).

Table 1. Uncoded and coded levels for concentration of tinuvin and iron particles determined by the CCD and incorporated in active food packaging.

Essay	Variables	
	Tinuvin 326 (% w/w)	Iron particles (% w/w)
1	0.07500 (-1)	2.2 (-1)
2	0.07500 (-1)	12.8 (+1)
3	0.42800 (+1)	2.2 (-1)
4	0.42800 (+1)	7.5 (0)
5	0.00189 (-1.41)	7.5 (0)
6	0.50111(+1.41)	7.5 (0)
7	0.25150 (0)	0.0047 (-1.41)
8	0.25150 (0)	15.0 (+1.41)
9	0.25150 (0)	7.5 (0)
10	0.25150 (0)	7.5 (0)
11	0.25150 (0)	7.5 (0)

2.3. Measurement of UV light absorption

The UV light absorption of developed films was determined by the measurement of the light transmitted through the samples. Measurement was done according to methodology described by COLTRO and BURATIN (2004). The percentage of the specular light transmission of the samples was determined using UV-Visible Spectrophotometer (GBC, Model 918, Melbourne, Victoria, Australia). The specular light transmission is the transmittance value obtained when measuring only the light transmitted in the same direction as the incident beam. The spectra were analyzed in the wavelength range of 200-700 nm at 120 nm/min scanning speed. In this measurement, the activity of developed films in the ultra violet region (wavelength below 400 nm), as well as in the visible region (wavelength greater than 400 nm) was monitored. Film samples had dimensions of 4 * 4 [cm.sup.2].

2.4. Film Characterization

2.4.1 X-ray diffraction (XRD)

The diffraction patterns of the UV barrier films were taken with the X-ray Diffraction System model X'Pert PRO (PANalytical, Netherland), using an iron filter and Co-K[alpha] radiation ([lambda] = 1.78890 [degrees]A). The diffraction pattern was obtained at diffraction angles between 10[degrees] and 80[degrees] (2[theta]).

2.5. Film thickness

The thicknesses of the samples were determined using a manual micrometer (0.01 mm, Mitutoyo, Suzano, Sao Paulo, Brazil). The average film thickness was calculated from the measurement of 10 points randomly selected on each film in triplicate. Mean values were used for the calculation of film properties when necessary.

2.6. Mechanical properties

Mechanical properties of the UV barrier films, including tensile strength at break, load at break and elongation at break, were measured according to standard method ASTM D882-02 (ASTM, 2012) using an Instron Universal Testing Machine (Model 3367, Instron Corporation, Norwood, MA, USA). The Instron was equipped with a load cell of 1 kN, with an initial grip separation of 50 mm and 500 mm/min speed. Sample dimension was 25 mm * 100 mm and the test was repeated 10 times for each treatment to confirm the repeatability.

2.7. Microscopic characterization

Morphological analysis of the UV barrier films was directly observed by scanning electron microscope (SEM, Hitachi TM--3000 Tabletop Microscope, Japan). Also, the surface of developed films was studied using Atomic Force Microscopy (AFM, NT-MDT, Russia). The AFM images were acquired in an intermittent contact mode at random areas of 100 * 100 [micro]m2. Samples were analyzed in triplicate at room temperature

(25[degrees]C).

2.8. Thermogravimetric analysis

This analysis was performed in a thermogravimetric analyzer (TGA-1000, Navas Instrument Conway, SC, USA). Samples of each UV absorber film (1 g approx.) were heated to 950[degrees]C at a heating rate of 10[degrees]C/min under nitrogen atmosphere. Weight losses of samples were measured as a function of temperature.

2.9. Color measurement

The color of the UV barrier films was measured with a colorimeter (COLORQUEST XE HunterLab, Reston, VA, USA). Measurements were done using the CIELAB scale, where each measurement is expressed as [L.sup.*] (indicating the brightness), [a.sup.*] (indicating red in the positive direction and green in the negative direction) and [b.sup.*] (indicating yellow in the positive direction and blue in the negative direction). Calculations were made for D-65 illuminant and 10[degrees] observation interval according to ASTM method E308 (ASTM, 2008). Opacity (OP) was calculated using the normalized values of the white background ([L.sup.*] = 93.44; [a.sup.*] = -0.63; [b.sup.*] = 1.21). In addition, the yellowness index (YIE313) and whiteness index (WI E313) were obtained using the Universal software V4.10 according to ASTM method E313-10 (ASTM, 2010). All color measurements were repeated three times.

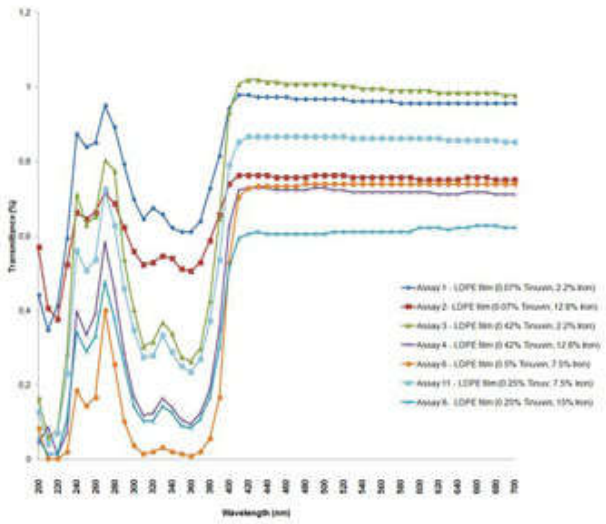

Figure 1. Spectrophotometric analysis of UV light absorption of various developed films.

3. RESULTS AND CONCLUSIONS

3.1. Measurement of UV Light Absorption

The effectiveness of the potential barrier to UV light of packaging material was analyzed considering that the UV light absorption is inversely proportional to transmitted light in the wavelength range varying from 200 to 400 nm. The spectrophotometric analysis showed that UV barrier films at high concentrations of tinuvin presented lower percentage of transmittance in the range of 200 to 400 nm (Fig. 1).

Three main wavelengths, 250 nm (UV-C), 310 nm (UV-B) and 360 nm (UV-A) were selected in order to analyze the results statistically. In all these three main wavelengths the measured absorption of UV light differed among treatments of the developed films with statistical significance and non-significant lack of fit (Table 2). In all three main wavelengths, the linear effect of tinuvin was significant, indicating that increasing

concentrations of tinuvin resulted in higher barrier to UV light. In addition, the quadratic effect of tinuvin was significant for UV light absorption when measured at 360 nm. On the other hand, the incorporation of iron particles had no significant effect on UV light absorption. Thus, the analysis of coefficients related to the spectrophotometric analysis at the three main wavelengths showed that the UV barrier films presented low percentage of transmittance in the range of 200 to 400 nm with increasing concentrations of tinuvin.

3.2. X-Ray Diffraction (XRD)

Crystallographic structure, chemical configuration and physical features of a material are provided by the XRD technique, in which the X-ray beam reaches the sample and is diffracted in a specific direction. Thus, the diffraction pattern is generated and it is considered a fingerprint of the analyzed sample. This technique is widely used because is nondestructive and the process of sample preparation is relatively simple (LUYKX et al., 2008). The pure iron particles, the control film (without additives) and the UV barrier films in the experiment were analyzed by XRD. The XRD patterns of iron particles and the control film are shown in Fig. 2.a. The sharp peak at 25.112[degrees] of 2[theta] value is assigned to LDPE, while the diffraction peak at 52.363[degrees] of 2[theta] corresponds to iron particles. The presence of iron in the developed films and its crystalline nature was confirmed by XRD analysis (Fig. 2.b). The UV barrier films incorporated with high concentrations of iron particles showed diffraction peak at 20 equal to 52.363[degrees], as observed in treatment No. 8 (15 % w/w iron) and No. 10 (7.5 % w/w iron), while the treatment No. 7 did not show this characteristic peak, due to low iron concentration in the film (0.01% w/w).

In addition, the characteristic peak of LDPE was observed in the XRD patterns indicating that the crystallinity of the LDPE was not affected by the incorporation of iron. The crystallinity degree and polymer orientation affect directly on physical and morphological structure, and these are considered as major factors in the permeability features of the film. In this way, the behavior of the crystalline regions, which serve as barrier, is significantly different from the behavior of the amorphous regions, where the permeability process takes place.

The incorporation of an oxygen absorber in films of LDPE resulted in decreased crystallinity, up to 20.73 %, in samples with 10 % additive (NOGUEIRA et al., 2005). This probably favored the permeability to gases and water vapor due to the increased space between the polymeric chains (WANG, 2001). These authors further reported that iron concentration did not affect the crystallinity of the UV barrier films.

3.3. Thickness and mechanical resistance

The thickness of developed UV barrier films presented no statistical difference among treatments. The developed films presented an average thickness of 0.13 mm, indicating that the incorporated compounds had no effect on this parameter. The mechanical properties of the films measure the material resistance before their rupture. The mechanical performance of the UV barrier films was evaluated by determining the maximum load (N), elongation at maximum load (%), elastic modulus (MPa), and tensile strength at maximum load (MPa). All measured properties differed among treatments and the regression model of tested properties presented statistical significance among developed films, with a non-significant lack of fit (Table 2).

These results indicated that the mechanical strength of LDPE films was affected after the incorporation of iron; however, tinuvin showed no influence on the mechanical properties of the UV barrier films. According to BRODY (2002), one of the biggest challenges of the production of active packaging, when incorporating active compounds to the polymeric matrix is the preservation of mechanical properties of the film. In this work, high concentrations of iron particles resulted in low values of maximum load. WURLITZER (2007) observed similar results after the incorporation of triclosan in polyvinylidene chloride (PVDC) matrix. Probably, these compounds occupied spaces in the polymeric matrix, large enough to create fatigue points which appeared in the polymer structure and resulted in reduced tensile strength.

The elongation at maximum load presented a behavior, in which the value of deformation decreased until a critical concentration of iron particles and beyond this point elongation at maximum load slightly increased. Stiffness of the material is measured by determination of the elastic modulus. In this work, UV barrier films presented a linear reduction of the elastic modulus. The reduction of tensile strength at maximum load of developed films related to increased iron concentration can be explained by the interaction between the resin

and iron particles embedded in the film.

The results of mechanical properties were consistent with microscopic observations, which showed agglomerations of iron particles likely to cause stress points, resulting in decreased mechanical resistance of the films.

3.4. Microscopic Characterization

Control film showed homogeneous surface, with the presence of some unmelted polymer resin (Fig. 3.a). On the other hand, tinuvin affected the morphology of UV barrier films and the incorporation of iron particles resulted in heterogeneous surface of developed films, as a result of protrusions promoted by agglomeration of iron particles (Figs. 3.b and 3.c). The AFM presented 3D images of developed films (Figs. 3.d-f). Such images confirmed the results observed by SEM, which showed the formation of unevenness on the surface of the films.

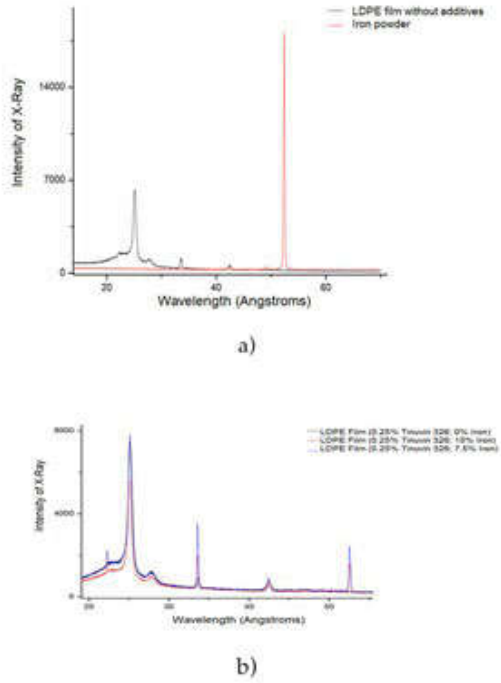

Figure 2. XRD patterns of: (a) iron particles and control film (without iron or tinuvin); and (b) UV barrier films with different concentrations of tinuvin and iron particles.

3.5. Thermogravimetric analysis

Dramatic temperature variations may lead to changes in packaging materials, influencing their thermal resistance. The thermal resistance of UV barrier films was studied by the thermogravimetric curve, which shows the mass loss of the sample in relation to the temperature. In general, the developed film showed extensive weight loss (>80%) at temperatures above 550[degrees]C (Fig. 4).

The thermal degradation of the films occurred in a single step, being initiated in the control film (LDPE) at 419[degrees]C and completed at 571[degrees]C. The thermal decomposition of developed films initiated at a lower temperature (370[degrees]C) and their thermal decomposition process was completed at 580[degrees]C.

The maximum temperature of films decomposition was calculated from the derivative of the thermogravimetric curve (data not shown). These results revealed that the average maximum temperature for

decomposition of control film was 552 [+ or -] 3[degrees]C while that for the UV barrier films was 550.1 [+ or -] 8[degrees]C.

3.6. Color Measurement

The color of packaging material is an important factor for the acceptance of food products (BOURTOOM and CHINNAN, 2008). In active food packaging, the active compounds bind to the polymeric matrix, resulting in changes in the natural film color (Rhim et al., 2000). Tinuvin and iron particles affected significantly the colorimetric parameters [L.sup.*], [a.sup.*], OP and WI (Table 2), while the YI and [b.sup.*] parameters were not influenced by them. The colorimetric parameters [L.sup.*] was influenced by the linear effect of iron particles ($p<0.05$), while the addition of tinuvin had no effect on this parameter. The linear regression coefficient for the concentration of iron particles was negative, which indicated that higher the concentration of the compound incorporated into the polymeric matrix resulted in low values of lightness in the films.

The colorimetric parameter [a.sup.*] was affected by the linear effect of tinuvin and iron particles. Linear effect of iron particles was positive, indicating that higher concentrations of iron results in higher values of [a.sup.*], a pronounced tendency to redness, while linear effect of tinuvin was negative, indicating that higher concentrations of tinuvin results in lower values of this parameter. The colorimetric parameter OP was affected only by the linear effect of iron, indicating that higher concentrations of iron particles result in more opaque films. This is in agreement with the results of the WI, which showed that higher concentrations of iron particles result in lower values of this colorimetric.

Finally, the incorporation of tinuvin and iron particles in low-density polyethylene allowed the development of new active packaging materials for food preservation. Results obtained from mechanical and physical characterizations of the developed films by incorporating tinuvin and iron showed the influence of these particles in the film performance. Furthermore, the incorporation of tinuvin resulted in significant absorption of UV light, while iron particles had no significant effect. Thus, this work leads to conclude that UV barrier films may be developed with the incorporation of tinuvin to control the oxidation process induced by light in food products.

ACKNOWLEDGMENTS

Financial support for this research was provided by CAPES (Coordenacao de Aperfeicoamento de Pessoal de Nivel Superior), CNPq (Conselho Nacional de Desenvolvimento Cientifico e Tecnologico) and the INCT (Instituto Nacional de Ciencia e Tecnologia) of Tropical Fruits in Brazil.

REFERENCES

ASTM 2008. ASTM E308--08. Standard practice for computing the colors of objects by using the CIE system. West Conshohocken, PA: ASTM International.

ASTM 2010. ASTM E313--10. Standard practice for calculating yellowness and whiteness indices from instrumentally measured color coordinates. West Conshohocken, PA: ASTM International.

ASTM 2012. ASTM D882. Standard test method for tensile properties of thin plastic sheeting. West Conshohocken: ASTM International.

Bourtoom T. and Chinnan M.S. 2008. Preparation and properties of rice starch-chitosan blend biodegradable film. LWT-Food Science and Technology, 41(9):1633-1641. DOI: dx.doi.org/10.1016/j.lwt.2007.10.014

Table 2. Estimated regression coefficients for measured physical-mechanical properties of UV absorber films incorporated with tinuvin and iron particles.

Term		Maximum load (N)	Elongation at maximum load (%)	Elastic modulus (MPa)	Tensile strength at maximum load (MPa)	L*	a*	OP	WI	250 nm (UV-C)	310 nm (UV-B)	360 nm (UV-A)
Mean		***29.78418***	***309.5723***	***74933.1***	***8884.194***	***84.96636***	***-0.72758***	***19.18455***	***57.2603***	***0.4906***	***0.293555***	***0.172253***
Tinuvin		-1.238174	-1.765508	-5545.558	-840.4226	0.6189114	***-0.113825***	-0.206873	0.7553746	***-0.16975***	***-0.21959***	-0.2261
Iron		***-3.205999***	-40.91711	***-10466.6***	***-1770.812***	***-6.292298***	***0.0727124***	***2.5879972***	***-13.39389***	-0.090734	-0.04383	-0.0387
Tinuvin^2		0.7753271	2.5020071	3979.814	375.4377	-0.663336	0.025764	0.3693061	-2.071671	0.045177	0.115384	***0.13258***
Iron^2		-2.01175	***-37.1685***	-405.9483	-542.3847	0.9883333	-0.025	-0.481667	2.5475	-0.0020476	-0.01154	-0.0091
Tinuvin × Iron		2.7925852	47.716964	7119.698	1337.3354	0.6950083	-0.011736	0.1059686	3.0025213	-0.0020476	-0.01583	-0.0159
Reg.	F^a	6.375988	7.241601	7.032227	9.596485	111.1178	40.25572	79.63881	58.10292	10.64317	19.98182	6.51794
	P^b	0.032497	0.01603	0.026397	0.012767	0.0001	0.0001	0.0001	0.0001	0.009801	0.001554	0.02092
Lack of fit	F^a	1.88709	0.294458	2.859416	1.706253	0.711301	0.511976	0.466179	1.41392	2.431165	6.250935	3.34449
	P^b	0.232769	0.755113	0.126599	0.264242	0.579851	0.777822	0.716495	0.327724	0.163244	0.02817	0.10572

Brody A.L. 2002. Action in active and intelligent packaging. Food Technology, 56(2):70-71.

Ciba 2002. Oxygen absorbers keep freshness in the package. Grenzach, Germany. Ciba Specialty Chemicals.

Coltro L. and Buratin A.E.P. 2004. Garrafas de PET para oleo comestivel: avaliacao da barreira a luz. Polimeros, 14206211.

Espitia P.J.P., Soares N.F.F., Coimbra J.S.R., Andrade N.J., Cruz R.S. and Medeiros E.A.A. 2012. Zinc oxide nanoparticles: Synthesis, antimicrobial activity and food packaging applications. Food and Bioprocess Technology, 5(5):1447-1464. DOI: doi.org/10.1007/s11947-012-0797-6

Faraoni A.S., Ramos A.M., Stringheta P.C. and Laureano J. 2008. Efeito dos metodos de conservacao, tipos de embalagem e tempo de estocagem na coloracao de polpa de manga "Uba" produzida em sistema organico. Revista Ceres, 55504-511.

Gibis D. and Rieblinger K. 2011. Oxygen scavenging films for food application. Procedia Food Science, 1(0):229- 234. DOI: dx.doi.org/10.1016/j.profoo.2011.09.036

Intawiwat N., Myhre E., 0ysad H., Jamtvedt S.H. and Pettersen M.K. 2012. Packaging materials with tailor made light transmission properties for food protection. Polymer Engineering & Science, 52(9):2015-2024. DOI: doi.org/10.1002/pen.23151

Lee D.S., Yam K.L. and Piergiovanni L. 2008. Food Packaging: Science and Technology, Boca Raton, CRC.

Luykx D.M.A.M., Peters R.J.B., Van Ruth S.M. and B ouwmeester H. 2008. A review of analytical methods for the identification and characterization of nano delivery systems in food. Journal of Agricultural and Food Chemistry, 56(18):8231-8247. DOI: doi.org/10.1021/jf8013926

Mortensen G., Bertelsen G., Mortensen B.K. and Stapelfeldt H. 2004. Light-induced changes in packaged cheeses--a review. International Dairy Journal, 14(2):85-102. DOI: dx.doi.org/10.1016 /S0958-6946(03)00169-9

Nogueira F.C.C., Sarantopoulos C.I.G.L. and Peres L. 2005. Estudo da cristalinidade em filme absorvedor de oxigenio para embalagens. Master in Chemical Engineering, UNICAMP.

Rhim J.W., Gennadios A., Handa A., Weller C.L. and Hanna M.A. 2000. Solubility, tensile, and color properties of modified soy protein isolate films. Journal of Agricultural and Food Chemistry, 48(10):4937-4941. DOI: doi.org/10.1021/jf0005418

Rodriguez-Rojas A., Arango Ospine A., Rodriguez-Velez P. and ARANA-FLOREZ R. 2019. ?What is the new

about food packaging material? A bibliometric review during 1996-2016. Trends in Food Science & Technology, 85252-261. DOI: doi.org/10.1016/j.tifs.2019.01.016

Sahraee S., Milani J.M., Regenstein J.M. and Kafil H.S. 2019. Protection of foods against oxidative deterioration using edible films and coatings: A review. Food Bioscience, 32100451. DOI: doi.org/10.1016 /j.fbio.2019.100451

Soares N.F.F. and Hotchkiss J.H. 1998. Bitterness reduction in grapefruit juice through active packaging. Packaging Technology and Science, 11(1):9-18.

Wang J. 2001. Design optimization of rigid metal containers. Finite Elements in Analysis and Design, 37(4):273- 286. DOI: dx.doi.org/10.1016/S0168-874X(00)00043-3

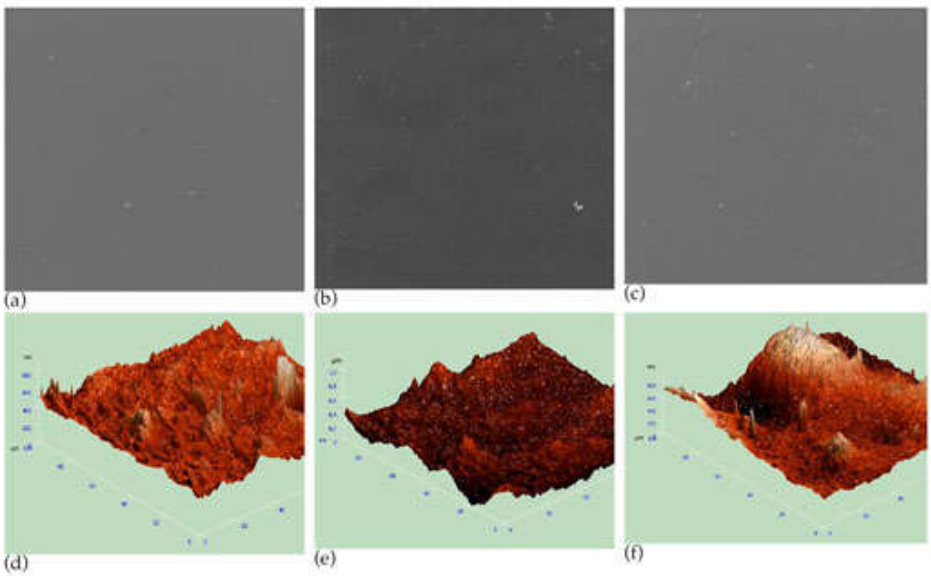

Figure 3. SEM* photomicrographs of control film (a), UV absorber films incorporated with the highest concentration of iron particles (15% w/w) (b) and highest concentration of tinuvin (0.5% w/w), as well as AFM photomicrographs of control film (d), UV absorber films incorporated with the highest concentration of iron particles (15% w/w) (e) and highest concentration of tinuvin (0.5% w/w) (f). *SEM images at 100X magnification.

Wurlitzer N.J. 2007. Desenvolvimento e avaliacao de propriedades antimicrobianas e fisicas de filme plastico incorporado com triclosan. Ph.D. in Food Science and Technology, Universidade Federal de Vicosa.

Yildirim S., Rocker B., Pettersen M.K., Nilsen-Nygaard J., Ayhan Z., Rutkaite R., Radusin T., Suminsk P., Marcos B. and Coma V. 2018. Active Packaging Applications for Food. Comprehensive Reviews in Food Science and Food Safety, 17(1):165-199. DOI: doi.org/10.1111/1541-4337.12322

R.A. BATISTA (1), J.T. FARIA (2), P.J.P. ESPITIA * (3), N. NARAIN (4), N.F.F. SOARES (5) and E. MEDEIROS (5)

(1) Instituto Tecnologico e de Pesquisa do Estado de Sergipe, Sergipe, Brasil

(2) Instituto de Ciencias Agrarias da Universidade Federal de Minas Gerais, Montes Claros, MG, Brasil

(3) Programa de Nutricion y Dietetica, Facultad de Nutricion y Dietetica, Universidad del Atlantico. Carrera 30 Numero 8-49 Puerto Colombia-Atlantico, Colombia

(4) Laboratorio de Flavor e Analise Cromatografico, Departamento de Tecnologia de Alimentos, Universidade Federal de Sergipe, Sergipe, Brasil

(5) Laboratorio de Embalagens, Departamento de Tecnologia de Alimentos, Universidade Federal de Vicosa, Vicosa, MG, Brasil

* E-mail address: perez.espitia@gmail.com; paulaperez@mail.uniatlantico.edu.co

Caption: Figure 1. Spectrophotometric analysis of UV light absorption of various developed films.

Caption: Figure 2. XRD patterns of: (a) iron particles and control film (without iron or tinuvin); and (b) UV barrier films with different concentrations of tinuvin and iron particles.

Caption: Figure 3. SEM * photomicrographs of control film (a), UV absorber films incorporated with the highest concentration of iron particles (15% w/w) (b) and highest concentration of tinuvin (0.5% w/w), as well as AFM photomicrographs of control film (d), UV absorber films incorporated with the highest concentration of iron particles (15% w/w) (e) and highest concentration of tinuvin (0.5% w/w) (f). * SEM images at 100X magnification.

Caption: Figure 4. TGA curve of UV barrier films with the maximum concentration of iron particles (15% w/w), highest concentration of tinuvin (0.5% w/w) and control film.

Table 1. Uncoded and coded levels for concentration of tinuvin and iron particles determined by the CCD and incorporated in active food packaging.

Essay	Variables	
	Tinuvin 326 (% w/w)	Iron particles (% w/w)
1	0.07500 (-1)	2.2 (-1)
2	0.07500 (-1)	12.8 (+1)
3	0.42800 (+1)	2.2 (-1)
4	0.42800 (+1)	7.5 (0)
5	0.00189 (-1.41)	7.5 (0)
6	0.50111(+1.41)	7.5 (0)
7	0.25150 (0)	0.0047 (-1.41)
8	0.25150 (0)	15.0 (+1.41)
9	0.25150 (0)	7.5 (0)
10	0.25150 (0)	7.5 (0)
11	0.25150 (0)	7.5 (0)

Table 2. Estimated regression coefficients for measured physical-mechanical properties of UV absorber films incorporated with tinuvin and iron particles.

Term		Maximum load (N)	Elongation at maximum load (%)
Mean		29.78418	309.5723
Tinuvin		-1.238174	-1.765508
Iron		-3.205999	-40.91711
Tinuvin2		0.7753271	2.5020071
Iron2		-2.01175	-37.1685
Tinuvin x Iron		2.7925852	47.716964
Reg.	[F.sup.a]	6.375988	7.241601
	[P.sup.b]	0.032497	0.01603
Lack	[F.sup.a]	1.88709	0.294458
of fit	[P.sup.b]	0.232769	0.755113

Term	Elastic modulus (MPa)	Tensile strength at maximum load (MPa)
Mean	74933.1	8884.194
Tinuvin	-5545.558	-840.4226
Iron	-10466.6	-1770.812
Tinuvin2	3979.814	375.4377
Iron2	-405.9483	-542.3847

Tinuvin x Iron		7119.698	1337.3354
Reg.	[F.sup.a]	7.032227	9.596485
	[P.sup.b]	0.026397	0.012767
Lack	[F.sup.a]	2.859416	1.706253
of fit	[P.sup.b]	0.126599	0.264242

Term		[L.sup.*]	[a.sup.*]	OP
Mean		84.96636	-0.72758	19.18455
Tinuvin		0.6189114	-0.113825	-0.206873
Iron		-6.292298	0.0727124	2.5879972
Tinuvin2		-0.663336	0.025764	0.3693061
Iron2		0.9883333	-0.025	-0.481667
Tinuvin x Iron		0.6950083	-0.011736	0.1059686
Reg.	[F.sup.a]	111.1178	40.25572	79.63881
	[P.sup.b]	0.0001	0.0001	0.0001
Lack	[F.sup.a]	0.711301	0.511976	0.466179
of fit	[P.sup.b]	0.579851	0.777822	0.716495

Term		WI	250 nm (UV-C)	310 nm (UV-B)
Mean		57.2603	0.4906	0.293555
Tinuvin		0.7553746	-0.16975	-0.21959
Iron		-13.39389	-0.090734	-0.04383
Tinuvin2		-2.071671	0.045177	0.115384
Iron2		2.5475	-0.0020476	-0.01154
Tinuvin x Iron		3.0025213	-0.0020476	-0.01583
Reg.	[F.sup.a]	58.10292	10.64317	19.98182
	[P.sup.b]	0.0001	0.009801	0.001554
Lack	[F.sup.a]	1.41392	2.431165	6.250935
of fit	[P.sup.b]	0.327724	0.163244	0.02817

Term		360 nm (UV-A)
Mean		0.172253
Tinuvin		-0.2261
Iron		-0.0387
Tinuvin2		0.13258
Iron2		-0.0091
Tinuvin x Iron		-0.0159
Reg.	[F.sup.a]	6.51794
	[P.sup.b]	0.02092
Lack	[F.sup.a]	3.34449
of fit	[P.sup.b]	0.10572

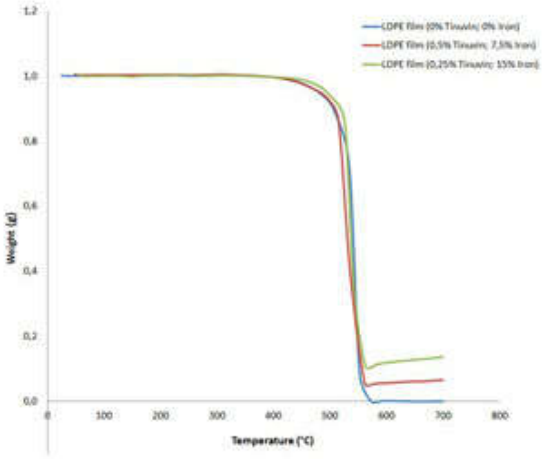

Figure 4. TGA curve of UV barrier films with the maximum concentration of iron particles (15% w/w), highest concentration of tinuvin (0.5% w/w) and control film.

Source Citation (MLA 9th Edition)

Batista, R.A., et al. "COMPOSITE FILMS AS ALTERNATIVE PACKAGING FOR UV-LIGHT BARRIER INTENDED FOR FOOD PRESERVATION." *Italian Journal of Food Science*, vol. 31, no. 6SI, Dec. 2019, pp. 1+. *Gale Academic OneFile*, link.gale.com/apps/doc/A623928058/AONE?u=ufmg_br&sid=googleScholar&xid=9def8443. Accessed 8 July 2022.

Gale Document Number: GALE|A623928058